Supplementary Information for

A sample-to-answer digital microfluidic multiplexed PCR system for syndromic pathogen detection in respiratory tract infection

Hao Bai, Jie Hu, Tangyuheng Liu, Liang Wan, Cheng Dong, Dasheng Luo, Fei Li, Zhanxin Yuan, Yunmei Tang, Tianlan Chen, Shan Wang, Hongna Gou, Yongzhao Zhou, Binwu Ying*, Jin Huang*, and Wenchuang (Walter) Hu*

*Corresponding author. Email: yingbinwu@scu.edu.cn (B. Ying); michael_huangjin@163.com (J. Huang); huwenchuang@wchscu.cn (W. Hu).

This file includes:

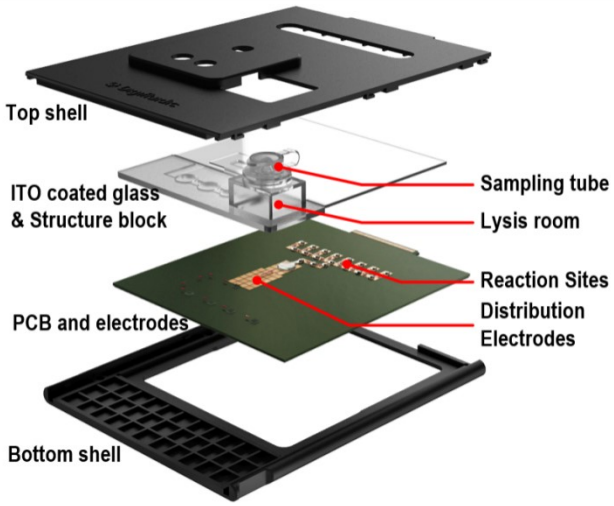

Fig. S1. The exploded structure views of the DMF chip. It includes top and bottom outer shells, ITO-coated cover glass plate and PC-made structure blocks, and PCB with electrodes.

(a)

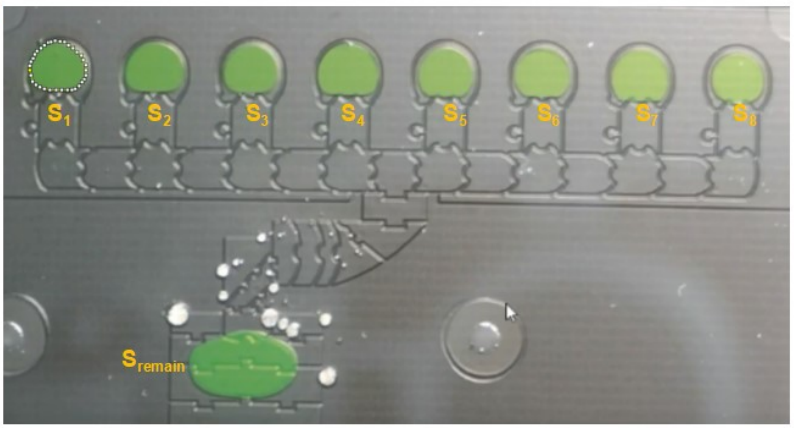

(b)

Results

File Edit Font Results

	Area	Mean	Min	Max
1	1805	113.211	71	198
2	1830	121.145	93	196
3	1820	132.031	97	196
4	1998	139.691	96	178
5	1837	150.919	98	209
6	1881	159.617	95	178
7	1983	167.820	139	190
8	1849	172.698	131	218
9	4783	117.753	74	194

Fig. S2. The calculation process of droplet volumes. (a) The outline image during the calculation of droplet volume. (b) The ImageJ software automatically calculates the number of pixels inside the outline.

Detailed calculation procedure is shown below:

1. Open ImageJ software and open one figure that contains the droplets to be calculated.
2. Select the "polygon selection" option from the toolbar.
3. Select all the droplets along its outline as depicted in Fig. S2a.
4. Obtain the number of pixels of the selected area as depicted in Fig. S2b, in this example, No. 1-8 is for the 8 smaller PCR reaction spots (S_1-S_8 in Fig. S2a) and No. 9 is for the big droplet at the bottom of the picture representing the remaining of elution buffer (S_{remain} in Fig. S2a).
5. We assume that the height of each droplet is the same, and the number of pixels of each droplet is directly proportional to the area of the corresponding droplet, so that the volume of the droplet is directly proportional to the number of pixels of the droplet.
6. The areas (in pixels) of the droplets at reaction points 1-8 are denoted as S_1-S_8 respectively, while the area (in pixels) of the remaining liquid is denoted as S_{remain}. The total area (total pixels) of the liquid is calculated and denoted as S_{total}. Since the total volume of all eluted liquid is known as 60 μL, the volume of the droplet in each reaction point (denoted as V_1-V_8) can be calculated as follows:

(1) $S_{total} = S_1 + S_2 + S_3 + S_4 + S_5 + S_6 + S_7 + S_8 + S_{remain}$

(2) $V_i = S_i/S_{total} * 60\ \mu L$, while i = 1, 2 , 3, ... 8

7. In this example,

$S_{total} = 1805 + 1830 + 1820 + 1998 + 1837 + 1881 + 1983 + 1849 + 4783 = 19786$

$V_1 = S_1 /S_{total} * 60\ \mu L = 1805/19786 * 60\ \mu L = 5.47\ \mu L$.

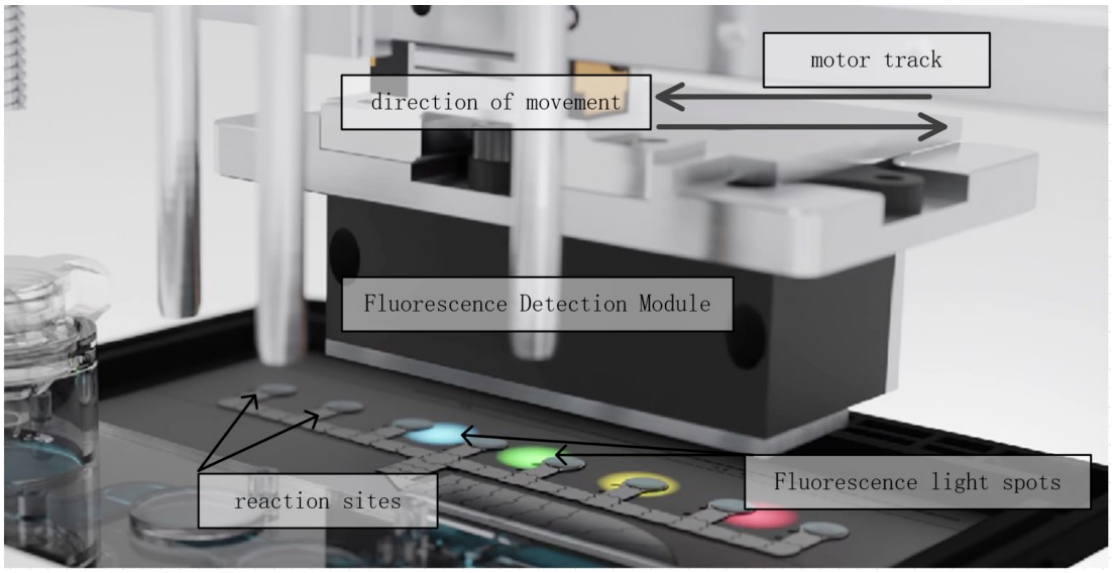

Fig. S3. The operation of 4-color fluorescence detection module.

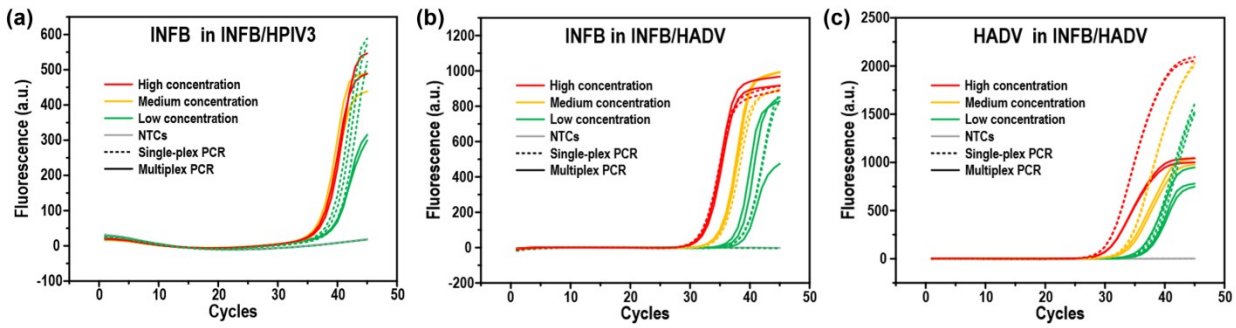

Fig. S4. Comparison of PCR amplification between single-plex and multiplex assays.

In the developing experiments of the INFB/HADV multiplex assay, the INFB was tested in combination with HADV and HPIV3. As Fig. S4a shows, in the multiplexing assay for the INFB and HPIV3, the efficiency of the INFB assay was deteriorated that only 2/3 samples were detected at low concentration (around the LOD concentration), while the single-plex INFB assay can detect 3/3 samples at low concentration. In comparison, in the multiplexing assay for the INFB and HADV, the LOD of the INFB can also detect 3/3 samples at low concentration (Fig. S4b). In addition, the efficiency of the HADV assay in the multiplex PCR was also comparable to the corresponding single-plex PCR (Fig. S4c). Therefore, the INFB assay was grouped with HADV. Several similar grouping experiments were conducted among the 15 single-plex assays. The optimal multiplex assay combinations were identified with neglectable compromise in PCR efficiency, fluorescence, and LOD.

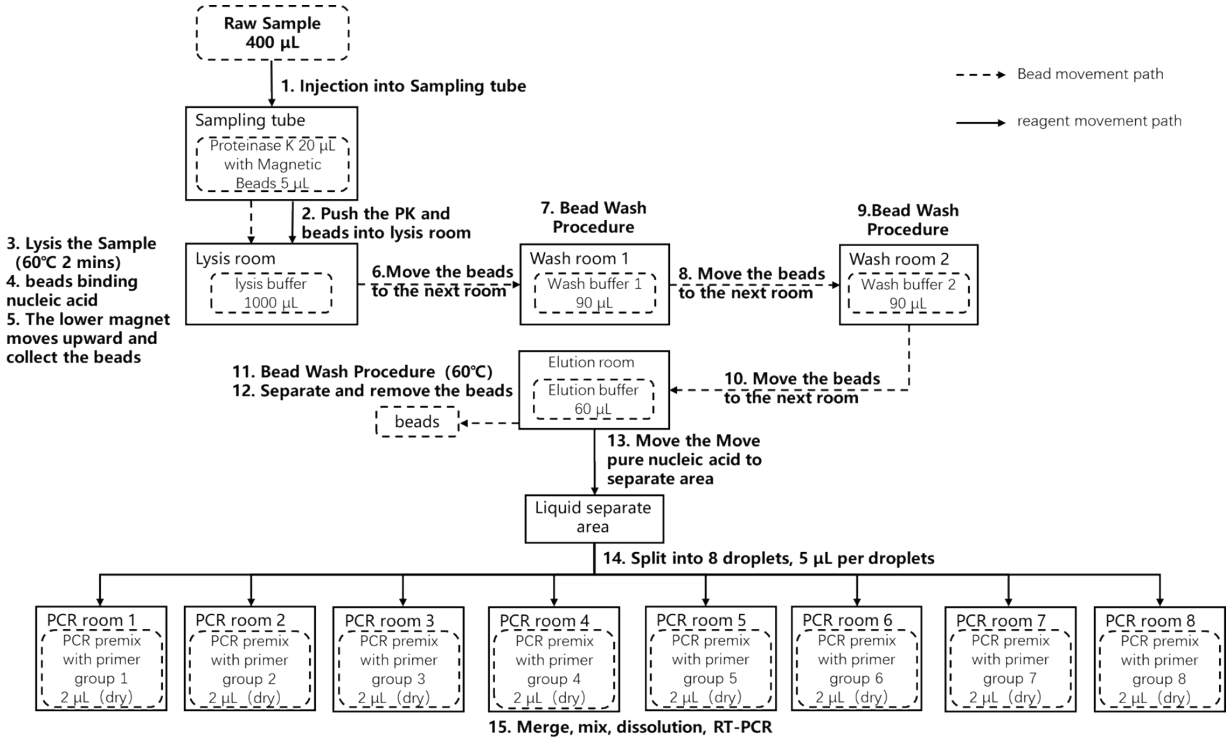

Fig. S5. The automatic workflow of the DMF chip from sample to result. Dash arrows denote the bead movement path; solid arrows denote the reagent movement path. Physical cavities are indicated by solid cells such as the sampling tube, lysis room, wash rooms, etc. Dotted boxes represent the reagents in the micro-chambers.

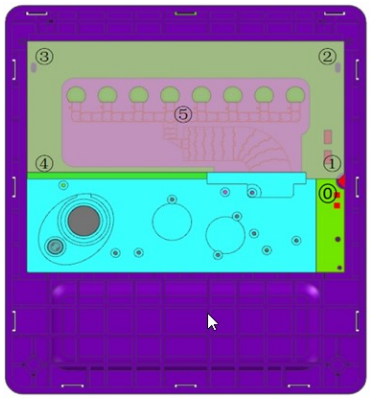

Fig. S6. The check points on the chip. Six check points were used for CPK calculation.

$$CPK = \frac{T}{6\sigma} \times (1 - \frac{\left| \bar{X} - \frac{max + min}{2} \right| \times 2}{T})$$

Where T is tolerance, $\bar{X}$ is the mean of the height, *max* and *min* represent the maximum and minimum height in the chip. The glue with standard height beads was used to replace the double adhesive tape, resulting in its CPK increasing to 1.37 from 0.86. The beads distribute the stress by multiple points which is better than the tape.

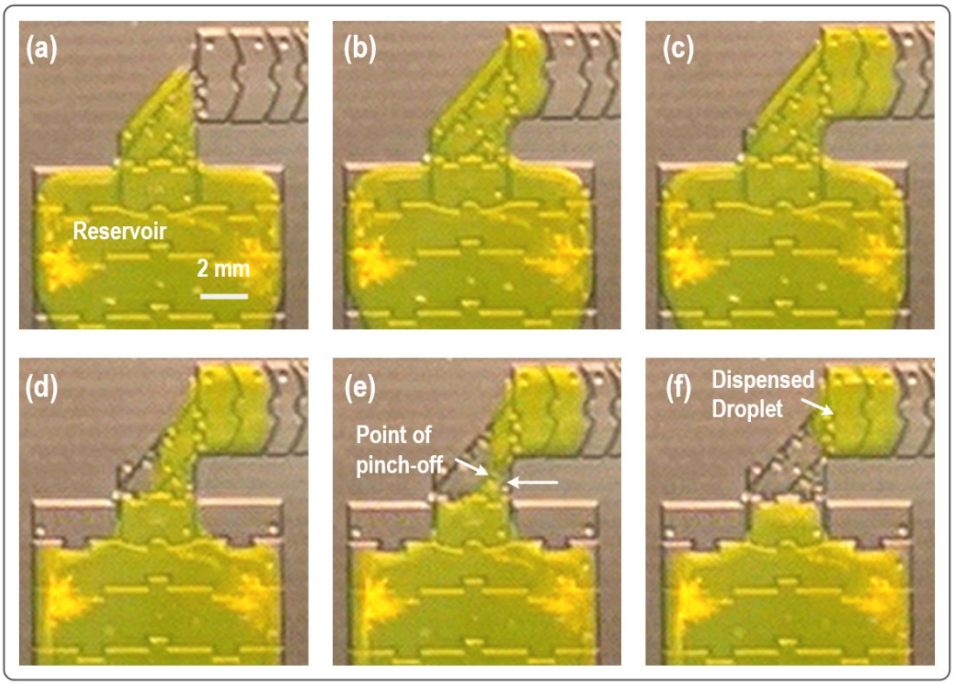

Fig. S7. Steps of droplet dispensing in L-junction electrode configuration. (a) Reservoir liquid gathered to enter the L-junction. (b-e) Liquid deformation by sequentially charging different electrodes with high voltage. (f) A daughter droplet was dispensed and ready to be moved to the reaction site.

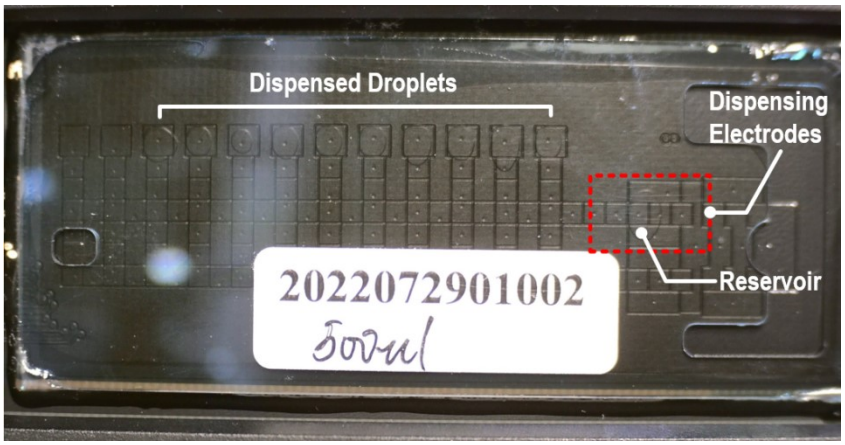

Fig. S8. Droplet dispensing by conventional droplet generation configuration.

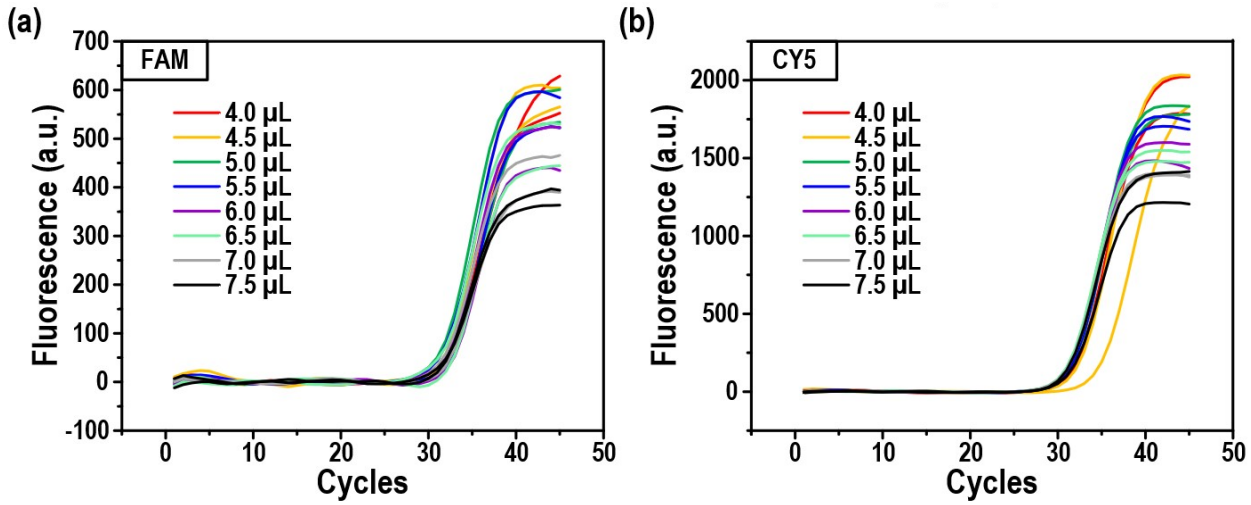

Fig. S9. Amplification curves of different reaction volumes for a) the FAM channel and b) the CY5 channel. The 2.3-µL reaction mixture was air-dry in PCR tubes. The purified nucleic acids of a bacterial strain Haemophilus influenzae (HI) and an armored RNA of Human Syncytial Virus (RSV) were mixed. Different volumes of the template mixture were added into the air-dried reaction tubes. Reactions were run in Gentier 96P Real-Time PCR System (TianLong Biotechnology, China). Thermal procedures consisted of 50 °C for 5 min, 95 °C for 20s, 45 cycles of 95 °C for 5 s, 58 °C for 20 s.

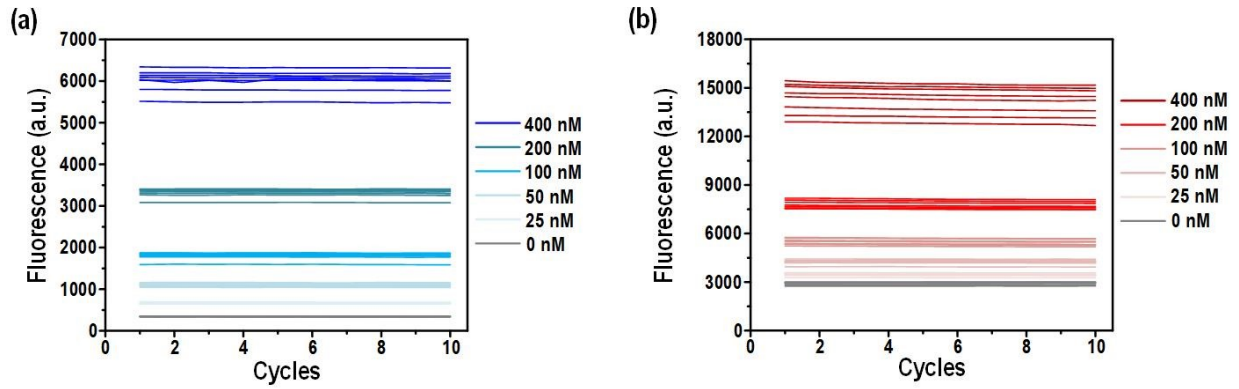

Fig. S10. The normalized fluorescence intensity for 6 different concentrations of a) FAM and b) CY5 fluorophore. The normalized fluorescence intensity was measured 10 times at each of the 8 reaction sites for 6 different concentrations of fluorescence dye. The CVs of the fluorescence intensity at each concentration (computed from each 800 data) were 3~5%.

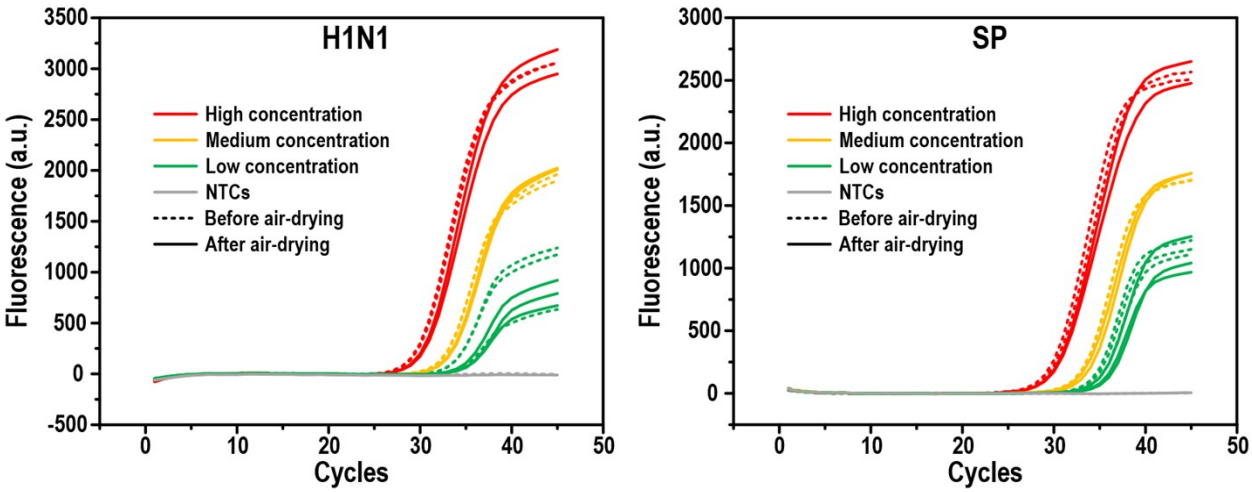

Fig. S11. Comparison of the PCR amplification before and after the air-drying step.

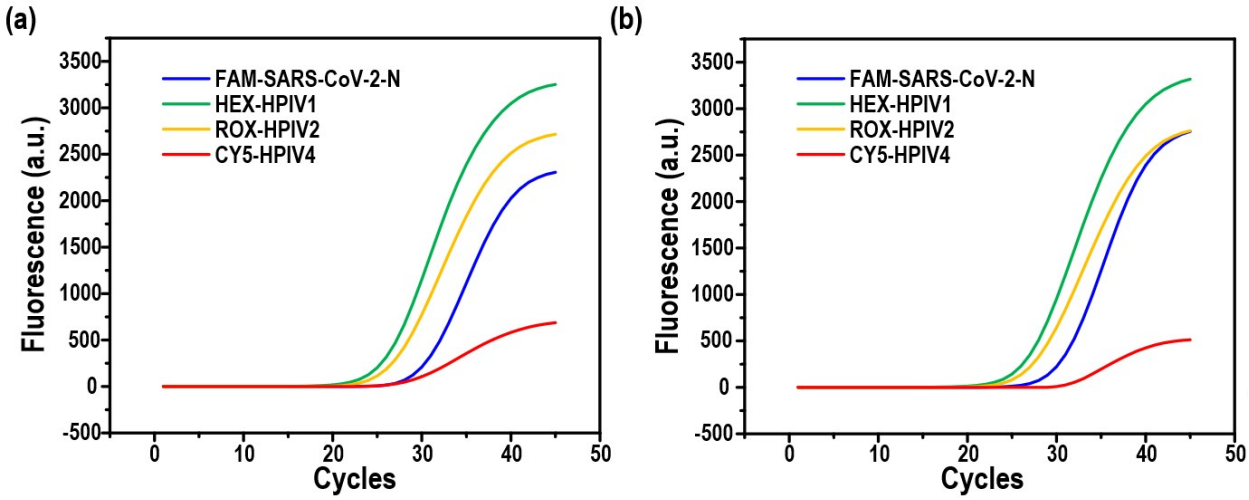

Fig. S12. Amplification curves for the 4-channel reactions. (a) Amplification curves for reaction 1. (b) Amplification curves for reaction 2.

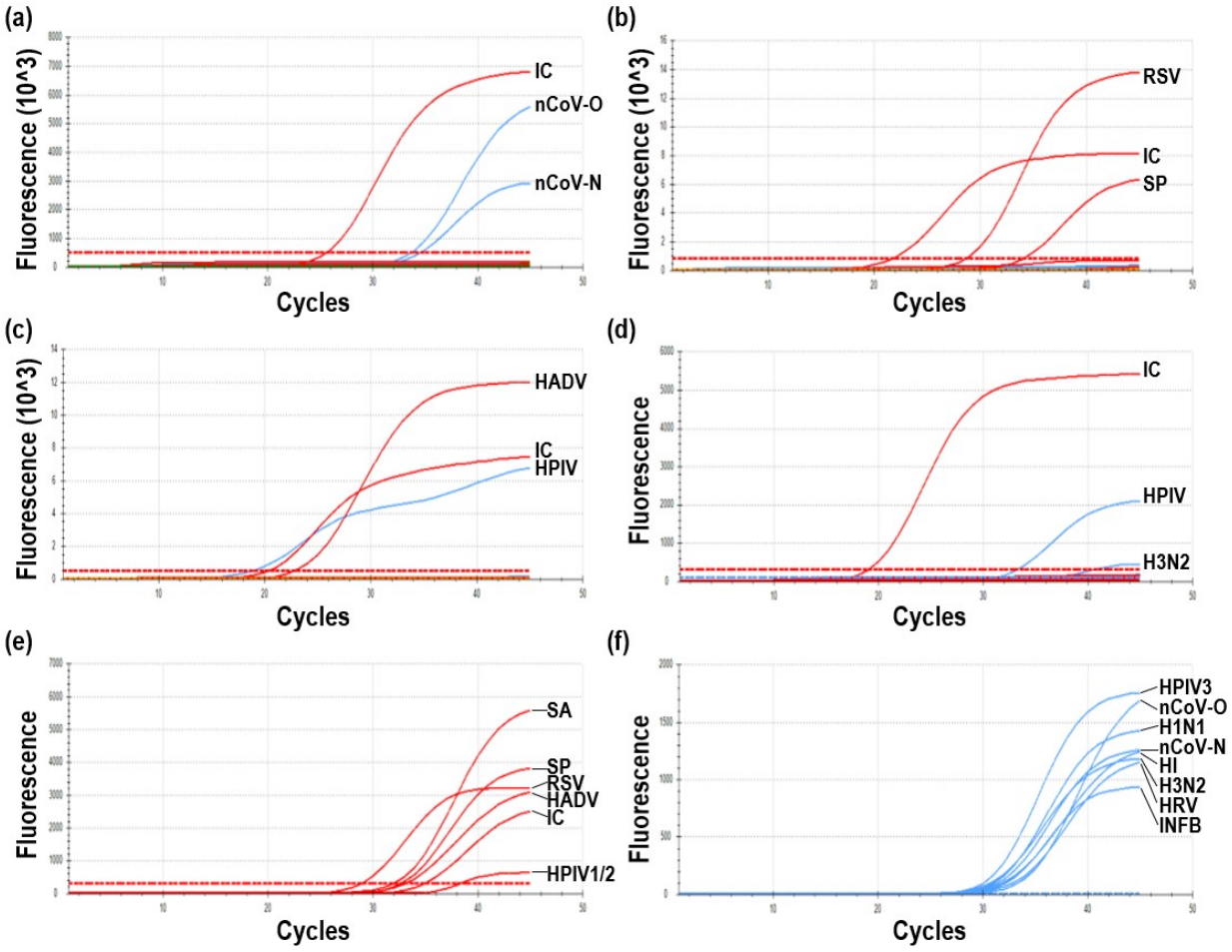

Fig. S13. Simultaneous detection of viral and bacterial pathogens in the clinical respiratory samples by the DMF assays. The amplification curves were generated by the in-house software. The Y axis indicates the fluorescent intensity, and the X axis indicates the amplification cycles. a-d) Results of amplifications of 4 clinical respiratory samples. e-f) Positive quality controls of the respiratory DMF assays for the e) CY5 channel and f) FAM channel.

Table S1. The simulation parameters of materials from the built-in library.

Parameters	Unit	PCB	Copper	Silicon glass	Mineral oil
Heat capacity at constant pressure	J/(kg*K)	1369	385	703	2090
Density	kg/m^3	1900	8960	2203	760
Heat conductivity coefficient	W/(m*K)	0.3	400	1.38	0.1

Table S2. Sequences of the primers and probes for the 15 respiratory pathogens.

Reaction	Sequence Name	Sequences 5'-3'	5'-end	3'-end
1	INFB-F	AGGCTTGTTGCTAAACTTGTTG	/	/
	INFB-R	TTCAGCTGCTCGAATTGGCTTT	/	/
	INFB-P	TGTCCTTCATTAAGACGCTCGAAGAGTGAG	FAM	BHQ1
	HADV-F	CGCTGGACATGACTTTTGAGGT	/	/
	HADV-R	CAGGTAGACGGCCTCGATGA	/	/
	HADV-P	TGGTGCACTCTGACCACGTCGAAGACTT	CY5	BHQ2
2	HPIV3-F	CAAGATCTACAAGTTGGCACAGCAA	/	/
	HPIV3-R	CATGGACATTCATTGTTTCCTGGTCT	/	/
	HPIV3-P	ACATTATGCCATGTCCATTTTATCC	FAM	Eclipse-MGB
3	H1N1-F	CTGGCCACAGGATTGAGGAATG	/	/
	H1N1-R	CTCTTCAGGTCGGCTGCATATC	/	/
	H1N1-P	ACCGTACCATCCATCTACCATCCCTGTCCA	FAM	BHQ1
	SP-F	TGGCTCTACTGTGAATTCTGGCT	/	/
	SP-R	TGGTACTACTTAGACGCTAAAGAAGGC	/	/
	SP-P	CGTCTGGTTTGAGGTAGTACCAGCCTGT	CY5	BHQ2
4	HRV-F1	TGTGCTCRCTTTGAGTCCTCC	/	/
	HRV-F2	TGTGCTTGATTGTGAGTCCTCC	/	/
	HRV-F3	TGTGCTACCAATGAGTCCTCC	/	/
	HRV-R	CGGACACCCAAAGTAGTYGGTC	/	/
	HRV-P	GCCCCTGAATGYGGCTAAYCTTAAMCC	FAM	BHQ1
	βA-F	ACGGTGAAGGTGACAGCAGT	/	/
	βA-R	TCCTGTAACAACGCATCTCATATTTGGA	/	/
	βA-P	ACAACAATGTGCAATCAAAGTCCTCGGCCAC	CY5	BHQ2
5	H3N2-F	CAGCAATCGATCAAATCAATGGGAA	/	/
	H3N2-R	CAAACAGTTTGTTCATTTCTGAGTCAGT	/	/
	H3N2-P	TTCTCCAGGGCAACAAGAAGCTCCGC	FAM	BHQ1
6	HI-F	CTCCGTTAATTTGGAGTGAAGAACTCG	/	/
	HI-R	GGGAATGATGCACCGTTAAAAGTACG	/	/

	HI-P	TCACAGCAACGCTGATACCCAACATACCCA	FAM	BHQ1
	RSV-F	GTGAACAARCTTCACGARGGC	/	/
	RSV-R1	TCTGCTGGCATGGATGATTGG		
	RSV-R2	TCTGCTGGCACAGATGACTG	/	/
	RSV-P	CACCCATATTGTAAGTGATGCAGGRTCATCGTC	CY5	BHQ3
	SARS-CoV-2-N-F	CTGGCAATGGCGGTGATG	/	/
	SARS-CoV-2-N-R	TGTTGTTGGCCTTTACCAGAC	/	/
	SARS-CoV-2-N-P	TTGCTGCTGCTTGACAGATTGAAC	FAM	BHQ1
	HPIV1-F	GGTGATGCAATATATGCGTATTCATCAA	/	/
	HPIV1-R	CCGGGTTTAAATCAGGATACATATCTGAA	/	/
7	HPIV1-P	TCACTCAAGGATGTGCAGATATAGGGAAGTCA	FAM	BHQ1
	HPIV2-F	CATGATGGGTGCAGAAGGTAGG	/	/
	HPIV2-R	AGGACGAGGAACTTGATAGGACG	/	/
	HPIV2-P	TACCCATTGAGCCTCAATGATCGGAGGAAT	FAM	BHQ1
	HPIV4-F	ACATCAATGCAGAATCATCTTATGATT	/	/
	HPIV4-R	GCGGGTCTATTGCATCAACTTC	/	/
	HPIV4-P	CTGCCAGAGCCCCAGATG	FAM	Eclipse-MGB
	SARS-CoV-2-O-F	GGTTTCACTACTTTCTGTTTTGCTT	/	/
	SARS-CoV-2-O-R	CAACTTCAGAATCACCATTAGCAAC	/	/
8	SARS-CoV-2-O-P	CTTTGTGAAGAAATGCTGGACAACAGGG	FAM	BHQ1
	SA-F	GTCCTGAAGCAAGTGCATTTACGA	/	/
	SA-R	CTTTAGCCAAGCCTTGACGAACTA	/	/
	SA-P	CCATCAGCATAAATATACGCTAAGCCACGTCC	CY5	BHQ2

Table S3. A three-day reproducibility test for the respiratory DMF chip.

Days	Chip No.	Channel	Site 1	Site 2	Site 3	Site 4	Site 5	Site 6	Site 7	Site 8
	1		28.33	29.78	29.00	26.61	29.65	26.91	28.30	29.00
	2		28.07	29.47	29.39	25.65	29.98	26.01	28.15	29.90
Day 1	3		28.04	29.43	28.91	26.27	30.23	25.76	27.64	29.13
	4		28.06	30.16	29.30	26.73	30.61	26.55	28.72	30.06
	5		28.10	29.61	28.90	27.26	31.97	27.07	28.51	29.21
	6		29.75	31.00	28.87	26.81	28.32	25.85	27.62	29.32
	7		29.77	30.78	28.61	26.35	28.91	26.03	28.03	29.42
Day 2	8	FAM	29.83	31.07	29.53	25.70	29.33	25.23	28.07	29.12
	9		30.31	30.70	29.90	26.15	29.17	26.13	28.53	29.39
	10		29.56	31.31	29.48	26.16	30.38	25.52	28.07	29.97
	11		28.53	30.27	29.44	25.83	28.68	24.83	27.44	28.08
	12		29.17	30.61	29.42	25.93	28.42	24.73	27.63	28.66
Day 3	13		29.35	31.08	29.6	26.04	28.95	25.4	28.34	29.27
	14		29.01	30.58	29.88	27.02	29.45	26.24	28.15	29.05
	15		29.35	31.03	29.56	26.96	28.98	25.98	27.85	29.61
	Ct-mean		29.02	30.46	29.32	26.36	29.54	25.88	28.07	29.28
	CV		2.65%	2.08%	1.30%	1.93%	3.28%	2.61%	1.34%	1.74%
Days	**Chip No.**	**Channel**	**Site 1**	**Site 2**	**Site 3**	**Site 4**	**Site 5**	**Site 6**	**Site 7***	**Site 8**
	1		27.95	-	27.82	28.85	-	27.20	25.17	27.43
	2		26.86	-	26.96	26.40	-	27.01	25.04	26.45
Day 1	3		26.90	-	27.08	27.33	-	26.79	24.80	25.84
	4		27.08	-	27.22	28.10	-	27.13	25.48	27.05
	5	CY5	28.20	-	27.94	28.78	-	27.19	25.45	27.57
	6		27.49	-	27.31	27.97	-	26.86	25.08	26.31
	7		26.72	-	26.60	27.31	-	27.06	25.10	26.64
Day 2	8		26.61	-	27.33	27.41	-	26.46	25.07	26.33
	9		27.38	-	27.55	26.99	-	27.27	25.25	26.86

	10		26.61	-	27.06	27.67	-	26.83	25.13	26.65
	11		26.29	-	26.64	26.64	-	25.28	24.47	25.06
	12		26.12	-	26.56	26.07	-	25.66	24.68	25.29
Day 3	13		27.22	-	26.92	28.92	-	26.14	25.11	25.93
	14		26.93	-	27.33	27.69	-	27.57	25.29	26.35
	15		27.25	-	27.27	27.58	-	26.96	25.23	26.55
	Ct-mean		27.04	-	27.17	27.58	-	26.76	25.09	26.42
	CV		2.10%	-	1.51%	3.12%	-	2.35%	1.07%	2.63%

*For the group 7, armoured RNA incorporating partial genomic sequences of HPIV-4 was utilized.

Table S4. Ct value for the 4-target reactions.

Channels	Reaction 1		Reaction 2	
	Target	Ct	Target	Ct
FAM	SARS-CoV-2-N	30.32	SARS-CoV-2-N	30.58
HEX	HPIV1	25.91	HPIV1	26.74
ROX	HPIV2	27.07	HPIV2	27.75
CY5	HPIV4	33.32	HPIV4	36.47